



2-7-2022

Functional Antagonism of WRI1 and TCP20 Modulates *GH3.3* Expression to Maintain Auxin Homeostasis in Roots

Que Kong
Nanyang Technological University, Singapore

Pui Man Low
Nanyang Technological University, Singapore

Audrey R. Q. Lim
Nanyang Technological University, Singapore

Yuzhou Yang
Nanyang Technological University, Singapore

Ling Yuan
University of Kentucky, lyuan3@uky.edu

See next page for additional authors

Follow this and additional works at: https://uknowledge.uky.edu/ktrdc_facpub



Part of the [Agriculture Commons](#)

Right click to open a feedback form in a new tab to let us know how this document benefits you.

Repository Citation

Kong, Que; Low, Pui Man; Lim, Audrey R. Q.; Yang, Yuzhou; Yuan, Ling; and Ma, Wei, "Functional Antagonism of WRI1 and TCP20 Modulates *GH3.3* Expression to Maintain Auxin Homeostasis in Roots" (2022). *Kentucky Tobacco Research and Development Center Faculty Publications*. 26.
https://uknowledge.uky.edu/ktrdc_facpub/26

This Article is brought to you for free and open access by the Tobacco Research and Development at UKnowledge. It has been accepted for inclusion in Kentucky Tobacco Research and Development Center Faculty Publications by an authorized administrator of UKnowledge. For more information, please contact UKnowledge@lsv.uky.edu.

Functional Antagonism of WRI1 and TCP20 Modulates *GH3.3* Expression to Maintain Auxin Homeostasis in Roots

Digital Object Identifier (DOI)

<https://doi.org/10.3390/plants11030454>

Notes/Citation Information

Published in *Plants*, v. 11, issue 3, 454.

© 2022 by the authors. Licensee MDPI, Basel, Switzerland.


This article is an open access article distributed under the terms and conditions of the Creative Commons Attribution (CC BY) license (<https://creativecommons.org/licenses/by/4.0/>).

Authors

Que Kong, Pui Man Low, Audrey R. Q. Lim, Yuzhou Yang, Ling Yuan, and Wei Ma

Communication

Functional Antagonism of WRI1 and TCP20 Modulates *GH3.3* Expression to Maintain Auxin Homeostasis in Roots

Que Kong¹, Pui Man Low¹, Audrey R. Q. Lim¹, Yuzhou Yang¹, Ling Yuan² and Wei Ma^{1,*} 

¹ School of Biological Sciences, Nanyang Technological University, Singapore 637551, Singapore; quekong@ntu.edu.sg (Q.K.); puiman001@e.ntu.edu.sg (P.M.L.); limr0029@e.ntu.edu.sg (A.R.Q.L.); yuzhou001@e.ntu.edu.sg (Y.Y.)

² Kentucky Tobacco Research and Development Center, Department of Plant and Soil Sciences, University of Kentucky, Lexington, KY 40546, USA; lyuan3@uky.edu

* Correspondence: weima@ntu.edu.sg

Abstract: Auxin is a well-studied phytohormone, vital for diverse plant developmental processes. The *GH3* genes are one of the major auxin responsive genes, whose expression changes lead to modulation of plant development and auxin homeostasis. However, the transcriptional regulation of these *GH3* genes remains largely unknown. WRI1 is an essential transcriptional regulator governing plant fatty acid biosynthesis. Recently, we identified that the expression of *GH3.3* is increased in the roots of *wri1-1* mutant. Nevertheless, in this study we found that AtWRI1 did not activate or repress the promoter of *GH3.3* (*proGH3.3*) despite of its binding to *proGH3.3*. Cross-family transcription factor interactions play pivotal roles in plant gene regulatory networks. To explore the molecular mechanism by which WRI1 controls *GH3.3* expression, we screened an Arabidopsis transcription factor library and identified TCP20 as a novel AtWRI1-interacting regulator. The interaction between AtWRI1 and TCP20 was further verified by several approaches. Importantly, we found that TCP20 directly regulates *GH3.3* expression via binding to TCP binding element. Furthermore, AtWRI1 repressed the TCP20-mediated transactivation of *proGH3.3*. EMSAs demonstrated that AtWRI1 antagonized TCP20 from binding to *proGH3.3*. Collectively, we provide new insights that WRI1 attenuates *GH3.3* expression through interaction with TCP20, highlighting a new mechanism that contributes to fine-tuning auxin homeostasis.

Keywords: Arabidopsis; gene regulation; protein-protein interaction; transcription factor; WRI1; TCP20



Citation: Kong, Q.; Low, P.M.; Lim, A.R.Q.; Yang, Y.; Yuan, L.; Ma, W. Functional Antagonism of WRI1 and TCP20 Modulates *GH3.3* Expression to Maintain Auxin Homeostasis in Roots. *Plants* **2022**, *11*, 454. <https://doi.org/10.3390/plants11030454>

Academic Editors: Milan S. Stankovic, Paula Baptista and Petronia Carillo

Received: 11 January 2022
Accepted: 4 February 2022
Published: 7 February 2022

Publisher's Note: MDPI stays neutral with regard to jurisdictional claims in published maps and institutional affiliations.



Copyright: © 2022 by the authors. Licensee MDPI, Basel, Switzerland. This article is an open access article distributed under the terms and conditions of the Creative Commons Attribution (CC BY) license (<https://creativecommons.org/licenses/by/4.0/>).

1. Introduction

The phytohormone auxin (indole-3-acetic acid; IAA) plays a pivotal role in plant developmental processes, such as embryogenesis, organogenesis, shoot and root growth, and organ patterning [1–3]. The *Aux/IAA* (AUXIN/INDOLE-3-ACETIC ACID), *SAUR* (small, auxin-induced RNA), and *GH3* (Gretchen Hagen 3) are the major auxin responsive genes [2,4,5]. Changes in *GH3* gene expression affect the plant developmental processes, such as the growth of hypocotyl, root, and shoot [6–9]. The *GH3* gene family in Arabidopsis comprises 20 members [9]. Several *GH3* genes control the formation of IAA-amino acid conjugates which play roles in storing, transporting, compartmentalizing, and metabolizing auxins [7,10]. These findings suggest that GH3s are essential for mediating auxin homeostasis and auxin-associated growth responses [11,12]. A majority of the *GH3* gene promoters have been found to contain *cis*-acting auxin responsive elements (AuxREs) that are recognized by auxin response factors (ARFs) [2,4,13]. In addition, bZIP transcription factors (e.g., Arabidopsis bZIP11) have been found to bind the G-box-related element (GRE) in the *GH3* promoter to activate *GH3* expression [11,14].

2. Results and Discussion

We recently found that the *GH3.3* gene is upregulated in the roots of Arabidopsis *WRINKLED1* (*AtWRI1*) loss-of-function mutant (*wri1-1*) [15]. *WRI1* is a member of APETALA2 (AP2) transcription factor family, well known for transcriptional regulation of plant oil accumulation [16,17]. *WRI1* functions as a transcriptional activator of genes involved in oil biosynthetic pathways [18–21]. However, how *AtWRI1* regulates the expression of *GH3.3* is unclear. *AtWRI1* is differentially expressed in Arabidopsis embryo over other vegetative tissues. *AtWRI1* also displays significant expression in roots [15,16]. Interestingly, although *AtWRI1* is able to bind to *proGH3.3* [15], our dual-luciferase (LUC) transactivation assay showed that *AtWRI1* did not activate or repress the promoter of *GH3.3* (*proGH3.3*) (Supplementary Figure S1). We hence hypothesized that *AtWRI1* regulates the expression of *GH3.3* through the coordination with an alternative transcriptional regulator. To investigate the molecular mechanism by which *WRI1* controls *GH3.3* expression, we performed yeast-two-hybrid (Y2H) assay to screen an Arabidopsis transcription factor library [22], using truncated *AtWRI1* variants (*AtWRI1*^{1–306} and *AtWRI1*^{58–240}) as baits. The truncated *AtWRI1* variants as baits are necessary to avoid high transactivation activity mediated by the C-terminus of *AtWRI1* [23]. We identified a class I TEOSINTE BRANCHED1/CYCLOIDEA/PROLIFERATING CELL FACTOR (TCP) family transcription factor TCP20 as a previously unknown interacting partner of *AtWRI1*. We confirmed that *AtWRI1* physically interacts with TCP20 in yeast cells (Figure 1A). In the pull-down assays, His-tagged TCP20 was pulled down by the GST agarose-coupled *AtWRI1* (Figure 1B), providing further evidence for the interaction between *AtWRI1* and TCP20. To further validate the *AtWRI1*-TCP20 interaction in vivo, we conducted bimolecular fluorescence complementation (BiFC) assays by co-producing the split YFP fusions of the two proteins, nYFP-*AtWRI1* and cYFP-TCP20, in *Nicotiana benthamiana* leaves. We detected YFP fluorescence in leaf samples that co-produced nYFP-*AtWRI1* and cYFP-TCP20 (Figure 1C). Taken together, our results verified the physical interaction between *AtWRI1* and TCP20.

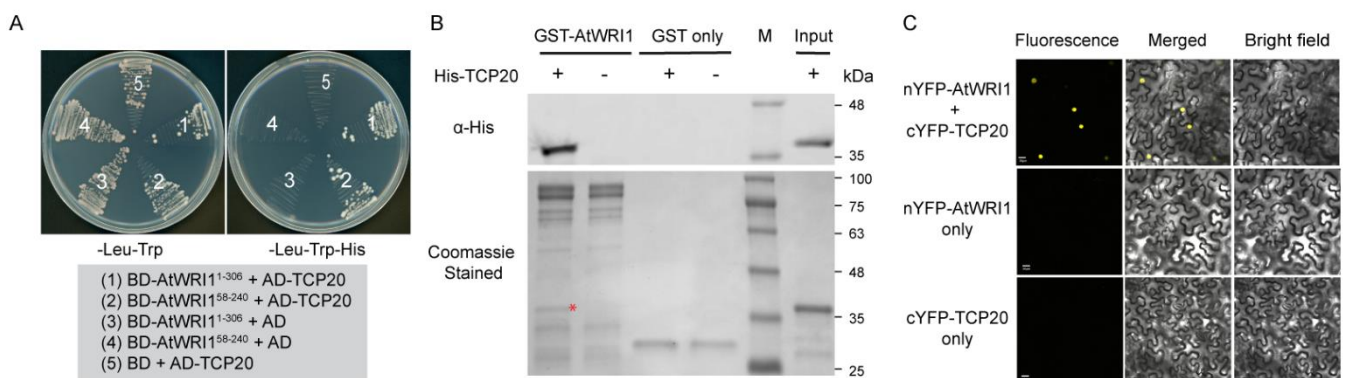


Figure 1. Physical interaction of *AtWRI1* with TCP20. **(A)** TCP20 interacts with *AtWRI1* variants in yeast cells. Yeast growth on either permissive (-Leu/-Trp) or stringent selective (-Leu/-Trp/-His) medium was shown. The numbers in the plates indicate the co-expression of DNA binding domain (BD) fusions of *AtWRI1* with varied amino acid length and activation domain (AD)-TCP20 fusion (indicated in shaded box). **(B)** GST pull-down assay showing the interaction of TCP20 with *AtWRI1*. The bottom panel shows Coomassie blue stained SDS-PAGE gel of GST pull-down using *E. coli* expressed protein. Red asterisk indicates the pull-down product of His-TCP20 that has identical molecular mass as the purified His-TCP20 in the far-right lane. The upper panel shows the immunoblotting of the pull-down products using anti-His antibody, verifying the presence of the His-TCP20. **(C)** A BiFC assay showing the physical interaction of *AtWRI1* with TCP20 in plant cells. Confocal images show *N. benthamiana* epidermal cells transiently co-producing nYFP-*AtWRI1* and cYFP-TCP20. Scale bar is 20 μ m.

Previous studies show that TCP20 is highly expressed in Arabidopsis roots to regulate numerous genes that are important for plant development and signaling pathways [24–26]. However, the molecular mechanism underlying TCP20 working with AtWRI1 to regulate *GH3.3* expression remains unknown. We thus analyzed *proGH3.3* and found four putative TCP binding motifs in the promoter (Supplementary Figure S2). To test whether TCP20 binds to *proGH3.3*, we synthesized four DNA probes (Probe 1–4), each containing an individual putative TCP binding motif with flanking sequences on both sides (Figure 2A and Supplementary Figure S2) and performed electrophoretic mobility shift assay (EMSA) using TCP20 protein. Our result showed that TCP20 bound to all four DNA probes (probe 1–4; Figure 2A); however, TCP20 failed to bind to the DNA probes with nucleotide mutations at the TCP20 binding element (probe 1M–4M; Figure 2A), implying the binding specificity to the TCP motifs in the *proGH3.3*. To explore the transcriptional regulation of *GH3.3* by TCP20, we subsequently characterized two homozygous Arabidopsis *tcp20* T-DNA insertional lines (*tcp20-2* (SALK_088460) and *tcp20-4* (SALK_041906)). We examined the expression of *GH3.3* in roots of *tcp20* loss-of-function mutants and found significant downregulation of *GH3.3* in both lines compared to wild-type (WT) (Figure 2B). We also examined the transactivation of TCP20 on *proGH3.3* using dual-LUC transient expression assay in *N. benthamiana* leaves (Figure 2C). TCP20 significantly activated the LUC expression driven by *proGH3.3* in the transient assay (Figure 2D). Taken together, these results indicate that TCP20 directly regulates *GH3.3* expression through binding to the TCP binding motifs in its promoter.

We next examined whether the transactivation activity of TCP20 on *proGH3.3* is attenuated by interaction with AtWRI1. The reporter vector, in which the LUC gene expression is driven by *proGH3.3*, was transformed into *N. benthamiana* leaves, alone or in combination with the effectors in which TCP20 or AtWRI1 is controlled by the CaMV 35S promoter (Figure 3A). While TCP20 significantly activated *proGH3.3*, the activation was greatly reduced when AtWRI1 was co-expressed (Figure 3B), suggesting that AtWRI1 antagonizes TCP20 upon the interaction. We also conducted a promoter deletion assay to identify the regions in *proGH3.3* critical for TCP20-AtWRI1 mediated expression. We generated three 5'-deletions in *proGH3.3-LUC* (Supplementary Figure S3). The full-length and truncated *proGH3.3-LUC* were transformed into *N. benthamiana* leaves alone, with AtWRI1, or with AtWRI1 and TCP20. The 1 kb deletion (from –1940 to –941 bp including one TCP binding motif) caused a significant reduction of LUC activity compared to the full-length promoter (Supplementary Figure S3). The 1.5 kb deletion (from –1940 to –441 bp) did not result in additional loss of activity compared to the 1 kb deletion. When all TCP binding motifs were deleted (–80 bp), less than 10% of the activity remained compared to the full-length promoter. In all cases except the –80 deletion, co-expression of TCP20 and AtWRI1 significantly reduced the transactivation of *proGH3.3* by TCP20 (Supplementary Figure S3). These results indicated that the deletion of motif 4 resulted in approximately 70% reduction of TCP20 activation, although the activation of the promoter fragment containing motifs 1–3 was still 15-fold higher than the reporter-alone control. Further removal of motifs 1–3 greatly reduced the activation and abolished the antagonizing effect of AtWRI1. Therefore, while motif 4 contributes most to the TCP20-mediated activation, all four TCP binding motifs contribute to the TCP20 regulation of *proGH3.3*. This conclusion is consistent with the EMSA results showing TCP20 binding to all four TCP binding motifs (Figure 2A).

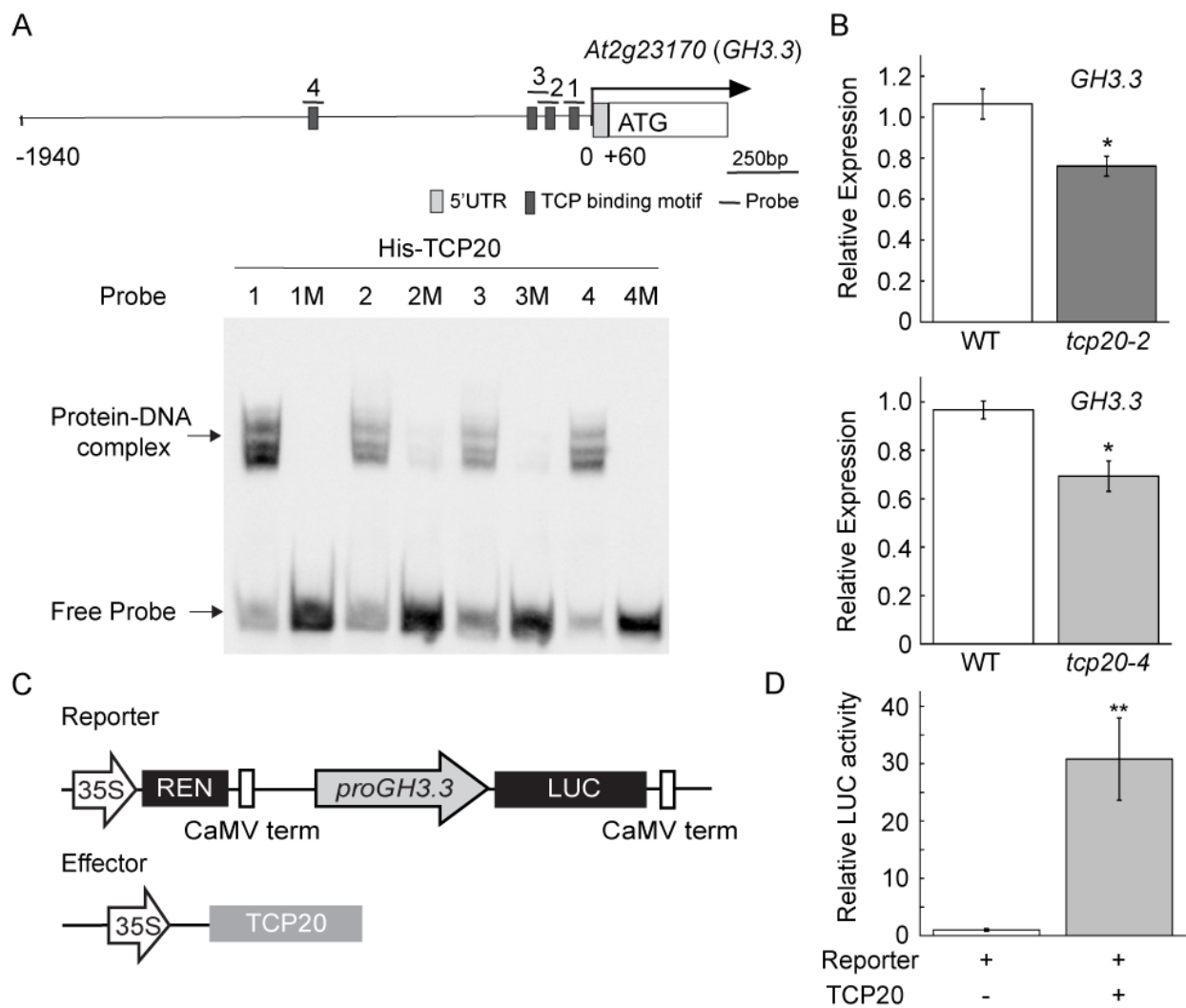


Figure 2. Direct promoter binding and regulation of *GH3.3* by TCP20. **(A)** EMSA showing TCP20 binding to the TCP binding motifs in the *GH3.3* promoter (*proGH3.3*). As indicated in the schematic representation of *proGH3.3*, four biotin-labelled DNA probes (dark boxes indicated by underlined numbers 1–4), containing consensus TCP binding motifs, and their corresponding mutant (M) probes (Supplementary Figure S2) were used for EMSA experiments to test the interaction with purified His-TCP20 protein. The shifted DNA-protein complexes are indicated by an arrow. **(B)** Quantitative real-time PCR (qRT-PCR) analysis of *GH3.3* transcript in the roots of wild-type (WT), *tcp20-2* (SALK_088460), and *tcp20-4* (SALK_041906) mutants. Results are shown as means \pm SE ($n = 3$). “*” indicates a significant difference ($p < 0.05$, Student’s *t*-test) compared with WT. **(C)** Schematic representation of the constructs used in a transient expression assay in *N. benthamiana* leaves. The *LUC* reporter gene was driven by a 2kb *proGH3.3*. The *Renilla* luciferase (*REN*) reporter gene was controlled by the *CaMV* 35S promoter. **(D)** Transactivation of the *LUC* reporter by TCP20 in *N. benthamiana* leaves. Relative reporter activity in *N. benthamiana*, infiltrated either using the reporter alone or in combination with the effector, was shown. The *LUC* activity was normalized to the *REN* activity. Results are shown as means \pm SE ($n = 5–6$). “***” indicates a significant difference ($p < 0.01$, one-way ANOVA) between reporter alone and co-transformation of TCP20 and reporter.

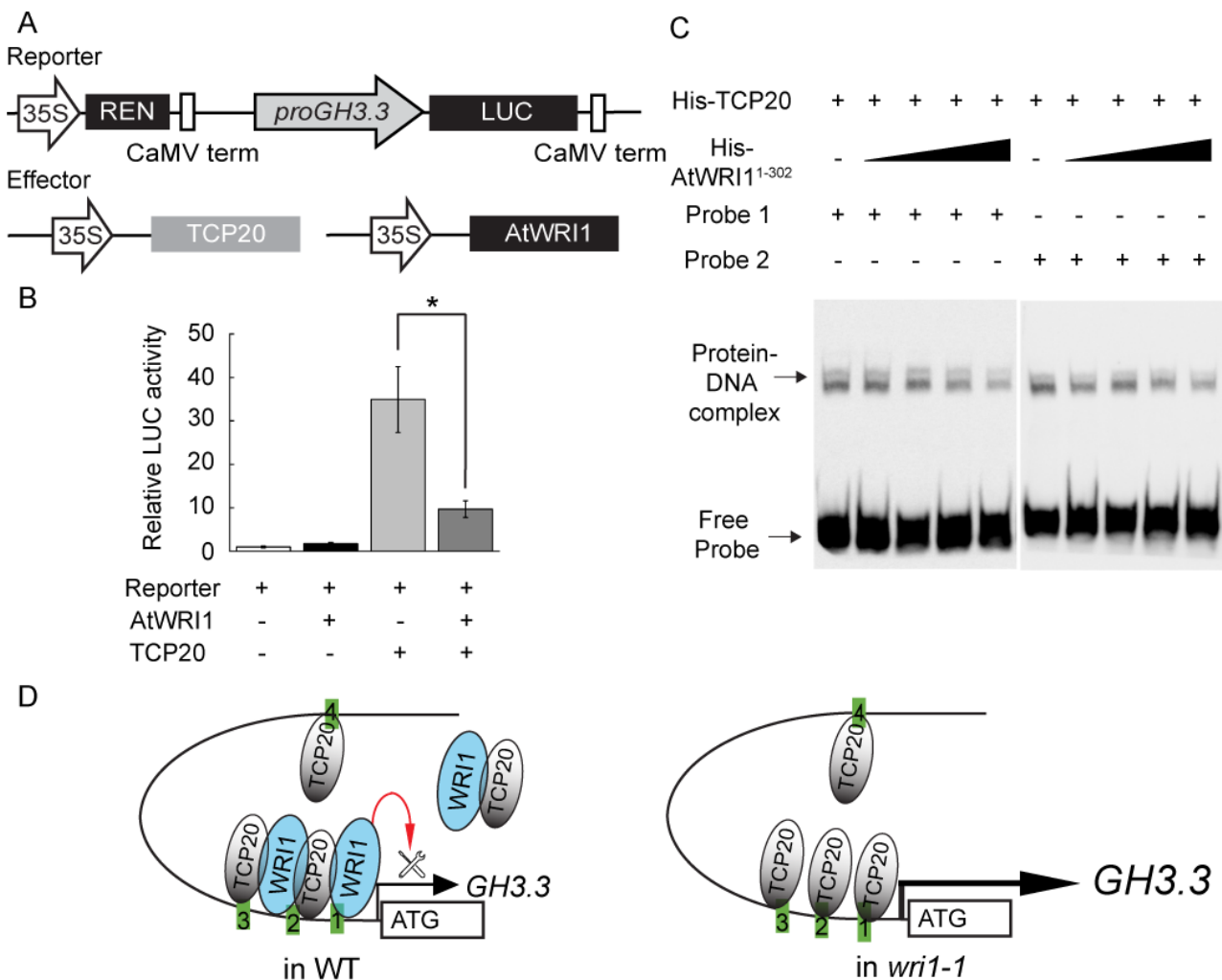


Figure 3. Interference of TCP20 binding to *proGH3.3* by AtWRI1. (A) Schematic representation of the constructs used in a transient expression assay in *N. benthamiana*. (B) Co-expression of AtWRI1 with TCP20 repressed the transactivation activity of TCP20 on *proGH3.3*. Results are shown as means \pm SE (n = 5–6). “*” indicates a significant difference ($p < 0.05$, Student’s t-test) between sole expression of TCP20 and co-expression of AtWRI1 with TCP20 as indicated. (C) EMSA demonstrated the TCP20 binding to *proGH3.3* fragments (probe 1 and 2; also see Supplementary Figure S2) in the presence of increasing amount of AtWRI1¹⁻³⁰² (0.53, 0.71, 1.06, and 2.12 pmol, respectively). The decreasing amount of the protein-DNA complex is indicated by an arrow. (D) A proposed model for co-regulation of *GH3.3* expression by TCP20 and WRI1. TCP20 activates *GH3.3* expression by direct binding to *proGH3.3*; however, the activation is attenuated by WRI1 through 1) co-occupation of the promoter and 2) formation of a possible non-DNA binding heterodimer. In any case, the TCP20-AtWRI1 complex exhibits reduced TCP20 target transactivation activity because of the TCP20-AtWRI1 interaction. Hence, in WT, WRI1 fine-tunes TCP20 activation of *GH3.3*, whereas in *wri1-1* that lacks WRI1, TCP20 exhibits stronger activation of *GH3.3* (represented by thicker arrow and increased size of *GH3.3*) compared to WT.

We demonstrated AtWRI1 attenuating the TCP20 activity on *proGH3.3* possibly by interacting sequestering TCP20. Our previous work shows the binding of AtWRI1 to *proGH3.3*. Additionally, WRI1 did not activate or repress *proGH3.3* in a transactivation assay suggesting that WRI1 likely requires a partner to function [15]. We therefore investigated whether AtWRI1 antagonizes TCP20 from binding to *proGH3.3* in EMSA. The results revealed that AtWRI1 bound to probes 1, 2, and 3 in a TCP binding site-independent manner, as AtWRI1 bound the mutant probes (1M, 2M, and 3M) with equal affinity as the

WT probes (Supplementary Figure S4). Since there is no recognizable WRI1 binding motif AW-box found in probes 1–3, AtWRI1 likely recognizes cryptic motifs that are close to the TCP binding motifs. Moreover, upon the addition of an increasing amount of AtWRI1¹⁻³⁰², we detected reduced binding of TCP20 to probe 1 and 2 (Figure 3C), but not probe 3 and 4 (Supplementary Figure S5A), in a dose-dependent manner (Supplementary Figure S5B). We therefore speculate that AtWRI1 antagonizes the function of TCP20 through two potential mechanisms: 1) both transcription factors co-occupy *proGH3.3*, resulting in reduced activity of TCP20, and 2) the AtWRI1-TCP20 heterodimer reduces the amount of free TCP20 to activate *proGH3.3* (Figure 3D). In the absence of AtWRI1, e.g., in *wri1-1* mutant, *GH3.3* is significantly upregulated (Figure 3D), leading to the increased production of IAA-Asp conjugates.

TCP20 is known to be involved in cell division, immunity, jasmonic acid biosynthesis, and nitrate foraging [27–29]. The regulation of auxin-responsive gene expression in this study defines a new role for TCP20 in Arabidopsis. Prior to this work, it was unclear how AtWRI1 affected auxin homeostasis through regulation of *GH3.3* expression. By demonstration of the direct binding of both AtWRI1 and TCP20 to *proGH3.3* and the protein-protein interaction of the two factors, we elucidate a previously unknown mechanism by which AtWRI1 antagonized the activity of TCP20 on *GH3.3* to modulate auxin homeostasis.

3. Materials and Methods

3.1. Plant Materials

Arabidopsis and *N. benthamiana* plants were grown in a growth chamber at 23 °C with a photoperiod of 16 h light (100–150 $\mu\text{mol m}^{-2} \text{s}^{-1}$ illumination)/8 h dark. Arabidopsis wild-type (Columbia ecotype) was used in this work. Seeds of the *tcp20-2* (SALK_088460) and *tcp20-4* (SALK_041906) mutants, which have been previously described [26], were obtained from the Arabidopsis Biological Resource Center (ABRC). Genotyping assay was conducted to confirm the homozygosity of *tcp20-2* and *tcp20-4* mutants. Reverse transcription-polymerase chain reaction assay was subsequently conducted to verify that the *TCP20* expression was disrupted in *tcp20-2* and *tcp20-4* mutants. Seed sterilization and germination were performed as previously described [30].

3.2. Bioinformatic Analysis

In silico analysis of TCP binding sites was performed using AthaMap [31].

3.3. Plasmid Construction

Entry constructs subcloning and recombination with destination vectors [Y2H vectors, BiFC vectors (pSITE-nEYFP-C1 and pSITE-cEYFP-C1 [32]), and pEarleyGate binary vectors [33] were via Gateway LR reactions (Life Technologies, Waltham, MA, USA). To generate constructs for epitope-tagged recombinant protein production in *E. coli*, the full-length *AtWRI1* and *TCP20* were sub-cloned into pET41a-GST and pET41a-6 \times His vectors, respectively, [34]. *AtWRI1*¹⁻³⁰² was sub-cloned into pNIC28-Bsa4 to produce an N-terminal 6 \times His-tagged protein (Protein Production Platform, Nanyang Technological University). To generate *proGH3.3:LUC* reporter constructs, various lengths of PCR amplified *proGH3.3* were subcloned into the pGreenII 0800-LUC vector [35]. A list of the primers used for plasmid construction in this study is provided in Table S1.

3.4. Yeast Two-Hybrid Assay (Y2H)

For screening Arabidopsis transcription factor library, transcription factors were sub-cloned into the pDEST22 vector (prey) and transformed into yeast strain Y187 (Clontech, San Jose, CA, USA). *AtWRI1* (*AtWRI1*¹⁻³⁰⁶ and *AtWRI1*⁵⁸⁻²⁴⁰) variants were sub-cloned into pDEST32 vector (bait) and introduced into yeast strain AH109. The prey and bait were mated and spotted on permissive (-Leu/-Trp) medium. After 3 days, the colonies were streaked onto stringent selective (-Leu/-Trp/-His) medium to screen positive interactions. *TCP20* was subcloned into pDEST22 as the prey and *AtWRI1* variants were subcloned into

pDEST32 as the bait. The prey and bait constructs were transformed into Y187 and AH109, respectively. Then the prey and bait were mated and plated on -Leu/-Trp medium. To evaluate the interaction, transformants were streaked onto stringent selective (-Leu/-Trp/-His) medium.

3.5. Transient Expression in *N. benthamiana*, BiFC, and Confocal Microscopy

For BiFC assay, *Agrobacterium tumefaciens* cells carrying the nYFP and cYFP fusion constructs were resuspended in MMA medium (10 mM MgCl₂, 10 mM MES, 100 μM acetosyringone) to an OD₆₀₀ of 1.2 and adjusted to an OD₆₀₀ of 0.4 before infiltration into *N. benthamiana* leaves. The plasmid pEAQ HT producing the P19 protein was co-infiltrated with other constructs to maintain high expression in *N. benthamiana* leaves [36]. Healthy leaves of *N. benthamiana* plants were infiltrated with *A. tumefaciens* suspensions carrying nYFP and cYFP fusion constructs using a 1 mL blunt-end syringe. After agroinfiltration, plants were placed in a growth chamber. YFP fluorescence signals were detected by a confocal microscope 2–3 days post agroinfiltration.

3.6. Recombinant Protein Production, In Vitro Pull-Down Assays, and EMSA

Recombinant proteins, including the GST-AtWRI1 variants and His-TCP20, were produced in *E. coli* strain BL21 (DE3). Protein induction, extraction and purification were conducted as described previously [23,34]. For in vitro pull-down assay, purified His-TCP20 protein was incubated with GST beads coupled with purified GST-AtWRI1 or GST protein in binding buffer [20 mM Tris-HCl (pH 7.4), 150 mM NaCl, 1 mM DTT, 0.1 mM EDTA (pH 8.0), 0.1% IGEPAL CA-630] at 4 °C overnight, followed by washing for 5 times with washing buffer (same as binding buffer). Then the samples were boiled in SDS-PAGE sample buffer at 95 °C for 5 min, followed by SDS-PAGE. The proteins were detected by immunoblot probed with anti-His antibody (Proteintech, Rosemont, IL, USA). EMSA was performed as described previously [34]. In brief, the 5' end biotin-labeled WT probes (1–4) and mutated probes (1M–4M) were used for EMSA. The standard binding reaction (20 μL) contained 0.05 μg/μL poly(dI-dC), 15 mM HEPES-KOH (pH 7.5), 7.5 mM KCl, 0.5 mM EDTA, 5% glycerol, 2 mM dithiothreitol, 1 μg/μL BSA, 2 fmol/μL of the hot DNA probe and ~1 pmol of His-TCP20. The binding competition assays were performed using ~1 pmol of His-TCP20 with addition of His-AtWRI1^{1–302} as described in the figure legend. The reaction mixture was incubated at room temperature for 30 min. The DNA-protein complexes were resolved on 5% (*w/v*) non-denaturing polyacrylamide gels and subsequently transferred to nylon membranes. The band shifts were detected by a chemiluminescent nucleic acid detection module (Thermo Fisher Scientific, Waltham, MA, USA).

3.7. RNA Extraction, Quantitative Real-Time PCR (qRT-PCR)

Roots from 1-week-old Arabidopsis seedlings grown vertically on the regular growth medium were harvested, immediately frozen in liquid nitrogen, and stored at –80 °C freezer until use for RNA extraction. Total RNA was extracted using the Monarch Total RNA Miniprep Kit (New England Biolabs, Ipswich, MA, USA) following the supplier's instructions. First-strand cDNA was synthesized using the qScript cDNA Synthesis Kit (Quantabio, Beverly, MA, USA). Quantitative real-time PCR (qRT-PCR) was conducted using Luna Universal qPCR Master Mix (New England Biolabs, Ipswich, MA, USA) according to the supplier's instructions. *Isopentenyl pyrophosphate:dimethylallyl pyrophosphate isomerase 2 (IPP2)* gene was used as an internal control to normalize the gene expression. The primers used for qRT-PCR is provided in Table S2.

3.8. Transient Dual-Luciferase (Dual-LUC) Assays

Transient dual-LUC assays in *N. benthamiana* were conducted as described previously [37,38], with minor modifications. After agroinfiltration, plants were placed in a plant growth chamber, and leaf samples were harvested 3 d after infiltration for the dual-LUC assay using Dual-Luciferase Reporter 1000 Assay System (Promega, Madison, WI, USA).

In brief, three leaf discs at agroinfiltration areas (5–6 mm in diameter) were excised and ground in liquid nitrogen to fine powder and homogenized in 100 µL Passive Lysis buffer (Promega, Madison, WI, USA). Subsequently, 5 µL of the extract was mixed with 40 µL Luciferase Assay Buffer, and the firefly LUC activity was measured by a cell imaging multi-mode plate reader (BioTek Cytation 5, Santa Clara, CA, USA). The reaction was stopped by addition of 40 µL Stop and Glo Buffer (Promega, Madison, WI, USA), and the Renilla (REN) LUC activity was measured. The firefly LUC activity was normalized to the REN LUC activity.

3.9. Accession Numbers

Accession numbers are as following: WRI1 (AT3G54320), TCP20 (AT3G27010), GH3.3 (AT2G23170).

Supplementary Materials: The following supporting information can be downloaded at: <https://www.mdpi.com/article/10.3390/plants11030454/s1>. Figure S1. Transactivation of the firefly luciferase (LUC) reporter by AtWRI1. Figure S2. In silico analysis of TCP binding sites in *proGH3.3*. Figure S3. The transactivation activity of TCP20 on the *proGH3.3* deletion fragments in *N. benthamiana* leaves. Figure S4. Examination of AtWRI1 binding to *proGH3.3* fragments that are also recognized by TCP20. Figure S5. Effects of AtWRI1 on TCP20 binding to *proGH3.3*. Table S1. Primers used for plasmid construction in this study. Table S2. Primers used for quantitative real-time PCR (qRT-PCR) in this study.

Author Contributions: Q.K. and W.M. conceived and designed the experiments. Q.K., P.M.L., A.R.Q.L. and Y.Y. performed the experiments. Q.K., L.Y. and W.M. analyzed the data. Q.K., L.Y. and W.M. wrote the manuscript. All authors have read and agreed to the published version of the manuscript.

Funding: This work was supported by a Nanyang Technological University Startup grant to W.M. and a Ministry of Education (MOE) of Singapore Tier 1 to W.M. (grant number: RG140/18).

Data Availability Statement: All data supporting the findings of this study are available within the paper and within its Supplementary Materials published online.

Acknowledgments: We thank Michael Thomashow (Michigan State University) for the Arabidopsis transcription factor library, Hao Yu and Chengxiang Li (National University of Singapore) for the vector of dual-luciferase assay, and Sitakanta Pattanaik (University of Kentucky) for critical reading of the manuscript. We also thank the NTU Protein Production Platform for His-AtWRI1¹⁻³⁰² protein expression and purification for the EMSA experiment.

Conflicts of Interest: The authors declare no conflict of interest.

References

1. Zhao, Y. Auxin biosynthesis and its role in plant development. *Annu. Rev. Plant Biol.* **2010**, *61*, 49–64. [[CrossRef](#)] [[PubMed](#)]
2. Woodward, A.W.; Bartel, B. Auxin: Regulation, action, and interaction. *Ann. Bot.* **2005**, *95*, 707–735. [[CrossRef](#)] [[PubMed](#)]
3. Lavy, M.; Estelle, M. Mechanisms of auxin signaling. *Development* **2016**, *143*, 3226–3229. [[CrossRef](#)] [[PubMed](#)]
4. Hagen, G.; Guilfoyle, T. Auxin-responsive gene expression: Genes, promoters and regulatory factors. *Plant Mol. Biol.* **2002**, *49*, 373–385. [[CrossRef](#)]
5. Paponov, I.A.; Paponov, M.; Teale, W.; Menges, M.; Chakrabortee, S.; Murray, J.A.; Palme, K. Comprehensive transcriptome analysis of auxin responses in Arabidopsis. *Mol. Plant* **2008**, *1*, 321–337. [[CrossRef](#)]
6. Nakazawa, M.; Yabe, N.; Ichikawa, T.; Yamamoto, Y.Y.; Yoshizumi, T.; Hasunuma, K.; Matsui, M. DFL1, an auxin-responsive GH3 gene homologue, negatively regulates shoot cell elongation and lateral root formation, and positively regulates the light response of hypocotyl length. *Plant J.* **2001**, *25*, 213–221. [[CrossRef](#)]
7. Park, J.E.; Park, J.Y.; Kim, Y.S.; Staswick, P.E.; Jeon, J.; Yun, J.; Kim, S.Y.; Kim, J.; Lee, Y.H.; Park, C.M. GH3-mediated auxin homeostasis links growth regulation with stress adaptation response in Arabidopsis. *J. Biol. Chem.* **2007**, *282*, 10036–10046. [[CrossRef](#)]
8. Khan, S.; Stone, J.M. Arabidopsis thaliana GH3.9 influences primary root growth. *Planta* **2007**, *226*, 21–34. [[CrossRef](#)]
9. Takase, T.; Nakazawa, M.; Ishikawa, A.; Manabe, K.; Matsui, M. DFL2, a new member of the Arabidopsis GH3 gene family, is involved in red light-specific hypocotyl elongation. *Plant Cell Physiol.* **2003**, *44*, 1071–1080. [[CrossRef](#)]
10. Staswick, P.E.; Serban, B.; Rowe, M.; Tiryaki, I.; Maldonado, M.T.; Maldonado, M.C.; Suza, W. Characterization of an Arabidopsis enzyme family that conjugates amino acids to indole-3-acetic acid. *Plant Cell* **2005**, *17*, 616–627. [[CrossRef](#)]

11. Weiste, C.; Droge-Laser, W. The Arabidopsis transcription factor bZIP11 activates auxin-mediated transcription by recruiting the histone acetylation machinery. *Nat. Commun.* **2014**, *5*, 3883. [[CrossRef](#)] [[PubMed](#)]
12. Chapman, E.J.; Estelle, M. Mechanism of auxin-regulated gene expression in plants. *Annu. Rev. Genet.* **2009**, *43*, 265–285. [[CrossRef](#)] [[PubMed](#)]
13. Guilfoyle, T.J.; Hagen, G. Auxin response factors. *Curr. Opin. Plant Biol.* **2007**, *10*, 453–460. [[CrossRef](#)] [[PubMed](#)]
14. Heinekamp, T.; Strathmann, A.; Kuhlmann, M.; Froissard, M.; Muller, A.; Perrot-Rechenmann, C.; Droge-Laser, W. The tobacco bZIP transcription factor BZI-1 binds the GH3 promoter in vivo and modulates auxin-induced transcription. *Plant J.* **2004**, *38*, 298–309. [[CrossRef](#)]
15. Kong, Q.; Ma, W.; Yang, H.; Ma, G.; Mantyla, J.J.; Benning, C. The Arabidopsis WRINKLED1 transcription factor affects auxin homeostasis in roots. *J. Exp. Bot.* **2017**, *68*, 4627–4634. [[CrossRef](#)] [[PubMed](#)]
16. Cernac, A.; Benning, C. WRINKLED1 encodes an AP2/EREB domain protein involved in the control of storage compound biosynthesis in Arabidopsis. *Plant J.* **2004**, *40*, 575–585. [[CrossRef](#)] [[PubMed](#)]
17. Kong, Q.; Ma, W. WRINKLED1 transcription factor: How much do we know about its regulatory mechanism? *Plant Sci.* **2018**, *272*, 153–156. [[CrossRef](#)]
18. Maeo, K.; Tokuda, T.; Ayame, A.; Mitsui, N.; Kawai, T.; Tsukagoshi, H.; Ishiguro, S.; Nakamura, K. An AP2-type transcription factor, WRINKLED1, of Arabidopsis thaliana binds to the AW-box sequence conserved among proximal upstream regions of genes involved in fatty acid synthesis. *Plant J.* **2009**, *60*, 476–487. [[CrossRef](#)]
19. Kong, Q.; Singh, S.K.; Mantyla, J.J.; Pattanaik, S.; Guo, L.; Yuan, L.; Benning, C.; Ma, W. TEOSINTE BRANCHED1/CYCLOIDEA/PROLIFERATING CELL FACTOR4 Interacts with WRINKLED1 to Mediate Seed Oil Biosynthesis. *Plant Physiol.* **2020**, *184*, 658–665. [[CrossRef](#)]
20. Baud, S.; Mendoza, M.S.; To, A.; Harscoet, E.; Lepiniec, L.; Dubreucq, B. WRINKLED1 specifies the regulatory action of LEAFY COTYLEDON2 towards fatty acid metabolism during seed maturation in Arabidopsis. *Plant J.* **2007**, *50*, 825–838. [[CrossRef](#)]
21. Kong, Q.; Yuan, L.; Ma, W. WRINKLED1, a “Master Regulator” in Transcriptional Control of Plant Oil Biosynthesis. *Plants* **2019**, *8*, 238. [[CrossRef](#)] [[PubMed](#)]
22. Kim, W.C.; Reza, I.B.; Kim, Y.; Park, S.; Thomashow, M.F.; Keegstra, K.; Han, K.H. Transcription factors that directly regulate the expression of CSLA9 encoding mannan synthase in Arabidopsis thaliana. *Plant Mol. Biol.* **2014**, *84*, 577–587. [[CrossRef](#)] [[PubMed](#)]
23. Ma, W.; Kong, Q.; Grix, M.; Mantyla, J.J.; Yang, Y.; Benning, C.; Ohlrogge, J.B. Deletion of a C-terminal intrinsically disordered region of WRINKLED1 affects its stability and enhances oil accumulation in Arabidopsis. *Plant J.* **2015**, *83*, 864–874. [[CrossRef](#)] [[PubMed](#)]
24. Herve, C.; Dabos, P.; Bardet, C.; Jauneau, A.; Auriac, M.C.; Ramboer, A.; Lacout, F.; Tremousaygue, D. In vivo interference with AtTCP20 function induces severe plant growth alterations and deregulates the expression of many genes important for development. *Plant Physiol.* **2009**, *149*, 1462–1477. [[CrossRef](#)]
25. Guan, P.; Ripoll, J.J.; Wang, R.; Vuong, L.; Bailey-Steinitz, L.J.; Ye, D.; Crawford, N.M. Interacting TCP and NLP transcription factors control plant responses to nitrate availability. *Proc. Natl. Acad. Sci. USA* **2017**, *114*, 2419–2424. [[CrossRef](#)] [[PubMed](#)]
26. Guan, P.; Wang, R.; Nacry, P.; Breton, G.; Kay, S.A.; Pruneda-Paz, J.L.; Davani, A.; Crawford, N.M. Nitrate foraging by Arabidopsis roots is mediated by the transcription factor TCP20 through the systemic signaling pathway. *Proc. Natl. Acad. Sci. USA* **2014**, *111*, 15267–15272. [[CrossRef](#)]
27. Lopez, J.A.; Sun, Y.; Blair, P.B.; Mukhtar, M.S. TCP three-way handshake: Linking developmental processes with plant immunity. *Trends Plant Sci.* **2015**, *20*, 238–245. [[CrossRef](#)]
28. Li, S. The Arabidopsis thaliana TCP transcription factors: A broadening horizon beyond development. *Plant Signal. Behav.* **2015**, *10*, e1044192. [[CrossRef](#)]
29. Danisman, S. TCP Transcription Factors at the Interface between Environmental Challenges and the Plant’s Growth Responses. *Front. Plant Sci.* **2016**, *7*, 1930. [[CrossRef](#)]
30. Ma, W.; Kong, Q.; Arondel, V.; Kilaru, A.; Bates, P.D.; Thrower, N.A.; Benning, C.; Ohlrogge, J.B. Wrinkled1, a ubiquitous regulator in oil accumulating tissues from Arabidopsis embryos to oil palm mesocarp. *PLoS ONE* **2013**, *8*, e68887. [[CrossRef](#)]
31. Steffens, N.O.; Galuschka, C.; Schindler, M.; Bulow, L.; Hehl, R. AthaMap web tools for database-assisted identification of combinatorial cis-regulatory elements and the display of highly conserved transcription factor binding sites in Arabidopsis thaliana. *Nucleic Acids Res.* **2005**, *33*, W397–W402. [[CrossRef](#)] [[PubMed](#)]
32. Martin, K.; Kopperud, K.; Chakrabarty, R.; Banerjee, R.; Brooks, R.; Goodin, M.M. Transient expression in Nicotiana benthamiana fluorescent marker lines provides enhanced definition of protein localization, movement and interactions in planta. *Plant J.* **2009**, *59*, 150–162. [[CrossRef](#)] [[PubMed](#)]
33. Earley, K.W.; Haag, J.R.; Pontes, O.; Opper, K.; Juehne, T.; Song, K.; Pikaard, C.S. Gateway-compatible vectors for plant functional genomics and proteomics. *Plant J.* **2006**, *45*, 616–629. [[CrossRef](#)] [[PubMed](#)]
34. Kong, Q.; Pattanaik, S.; Feller, A.; Werkman, J.R.; Chai, C.; Wang, Y.; Grotewold, E.; Yuan, L. Regulatory switch enforced by basic helix-loop-helix and ACT-domain mediated dimerizations of the maize transcription factor R. *Proc. Natl. Acad. Sci. USA* **2012**, *109*, E2091–E2097. [[CrossRef](#)] [[PubMed](#)]
35. Hellens, R.P.; Allan, A.C.; Friel, E.N.; Bolitho, K.; Grafton, K.; Templeton, M.D.; Karunairetnam, S.; Gleave, A.P.; Laing, W.A. Transient expression vectors for functional genomics, quantification of promoter activity and RNA silencing in plants. *Plant Methods* **2005**, *1*, 13. [[CrossRef](#)] [[PubMed](#)]

36. Sainsbury, F.; Thuenemann, E.C.; Lomonosoff, G.P. pEAQ: Versatile expression vectors for easy and quick transient expression of heterologous proteins in plants. *Plant Biotechnol. J.* **2009**, *7*, 682–693. [[CrossRef](#)] [[PubMed](#)]
37. Li, J.; Li, G.; Gao, S.; Martinez, C.; He, G.; Zhou, Z.; Huang, X.; Lee, J.H.; Zhang, H.; Shen, Y.; et al. Arabidopsis transcription factor ELONGATED HYPOCOTYL5 plays a role in the feedback regulation of phytochrome A signaling. *Plant Cell* **2010**, *22*, 3634–3649. [[CrossRef](#)]
38. Liu, H.; Yu, X.; Li, K.; Klejnot, J.; Yang, H.; Lisiero, D.; Lin, C. Photoexcited CRY2 interacts with CIB1 to regulate transcription and floral initiation in Arabidopsis. *Science* **2008**, *322*, 1535–1539. [[CrossRef](#)]